Accepted Manuscript

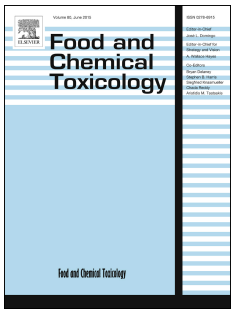

Evidence of insulin-dependent signalling mechanisms produced by *Citrus sinensis* (L.) Osbeck fruit peel in an insulin resistant diabetic animal model

Rajiv Gandhi Sathiyabama, Rajiv Gandhi Gopalsamy, Marina Denadai, Gurunagarajan Sridharan, Jothi Gnanasekaran, Sasikumar Ponnusamy, Jullyana de Souza Siqueira Quintans, Narendra Narain, Luis Eduardo Cuevas, Henrique Douglas Melo Coutinho, Andreza Guedes Barbosa Ramos, Lucindo José Quintans-Júnior, Ricardo Queiroz Gurgel

PII: S0278-6915(18)30199-6

DOI: 10.1016/j.fct.2018.03.050

Reference: FCT 9686

To appear in: *Food and Chemical Toxicology*

Received Date: 28 January 2018

Revised Date: 5 March 2018

Accepted Date: 30 March 2018

Please cite this article as: Sathiyabama, R.G., Gopalsamy, R.G., Denadai, M., Sridharan, G., Gnanasekaran, J., Ponnusamy, S., Siqueira Quintans, J.d.S., Narain, N., Cuevas, L.E., Coutinho, H.D.M., Ramos, A.G.B., Quintans-Júnior, Lucindo.José., Gurgel, R.Q., Evidence of insulin-dependent signalling mechanisms produced by *Citrus sinensis* (L.) Osbeck fruit peel in an insulin resistant diabetic animal model, *Food and Chemical Toxicology* (2018), doi: 10.1016/j.fct.2018.03.050.

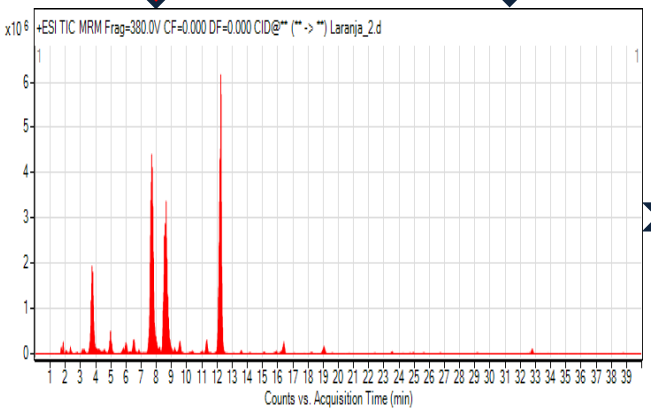

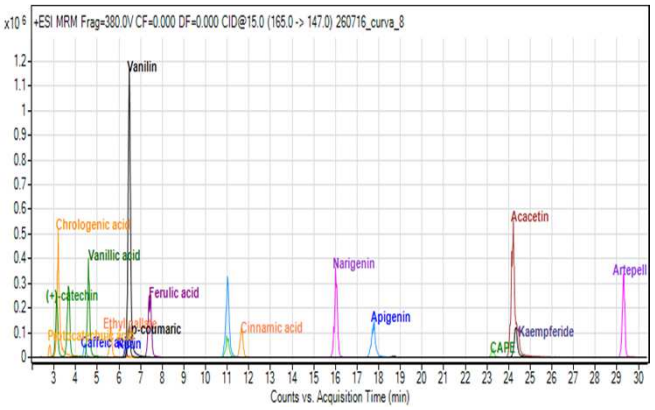

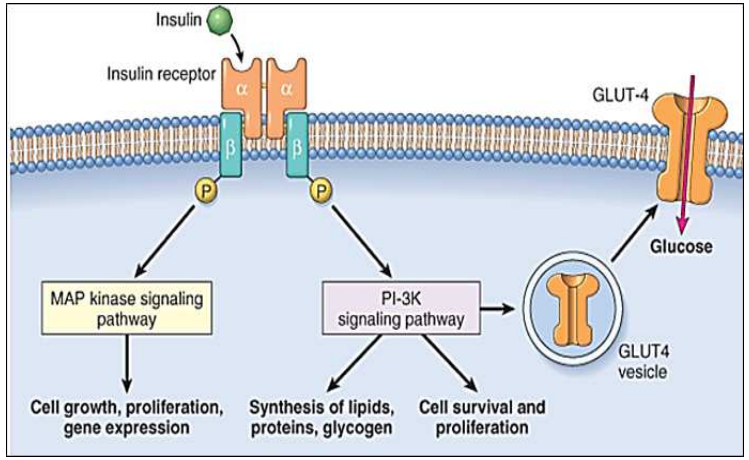

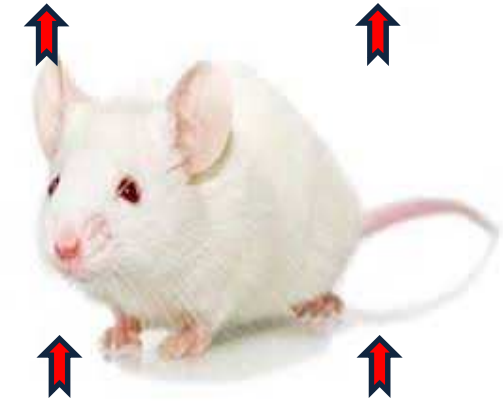

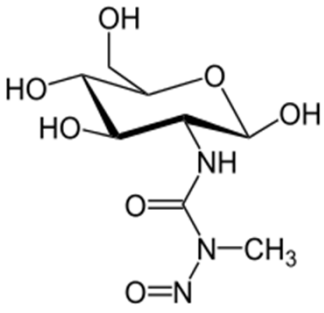

Streptozotocin

High Fat Diet

Insulin Resistant Diabetic Animal Model

Lowered Fasting Blood Glucose

Attenuated Insulin Resistance

Promoted Insulin Receptor Signalling

Evidence of insulin-dependent signalling mechanisms produced by *Citrus sinensis* (L.) Osbeck fruit peel in an insulin resistant diabetic animal model

Rajiv Gandhi Sathiyabama[a], Gopalsamy Rajiv Gandhi[a], Marina Denadai[b], Gurunagarajan Sridharan[c], Gnanasekaran Jothi[c], Ponnusamy Sasikumar[d], Jullyana de Souza Siqueira Quintans[e], Narendra Narain[b], Luis Eduardo Cuevas[f], Henrique Douglas Melo Coutinho[g], Andreza Guedes Barbosa Ramos[e], Lucindo José Quintans-Júnior[e, *], Ricardo Queiroz Gurgel[a, *]

[a] *Department of Medicine, Postgraduate Program in Health Sciences, Federal University of Sergipe, Rua Cláudio Batista, s/n, Cidade Nova, Aracaju, 49.100-000 Sergipe, Brazil.*

[b] *Laboratory of Flavor and Chromatographic Analysis, Federal University of Sergipe, São Cristóvão, 49.100-000 Sergipe, Brazil*

[c] *Department of Biochemistry, Srimad Andavan Arts and Science College, Tiruchirapalli, 620005 Tamil Nadu, India.*

[d] *Department of Oral Biology, University at Buffalo, New York 14214, USA.*

[e] *Laboratory of Neuroscience and Pharmacological Assays (LANEF), Department of Physiology, Federal University of Sergipe, São Cristóvão, 49.100-000, Sergipe, Brazil.*

[f] *Liverpool School of Tropical Medicine, Pembroke Place Liverpool, Liverpool, UK*

[g] *Laboratory of Microbiology and Molecular Biology, Department of Biological Chemistry, Regional University of Cariri, Crato-CE, Rua Cel, Pimenta 63.105-000, Brazil*

*Authors to whom correspondence should be addressed: *E-mails*: lucindojr@gmail.com (to LJQJ) or ricardoqgurgel@gmail.com (RQG), Federal University of Sergipe, Aracaju, 49.100-000 Sergipe, Brazil. Mobile.: +55-79-988015026; Fax: +55-79-3212-6640

Abbreviations: ALP, alkaline phosphatase; CAPE, caffeic acid phenyl ester; CSMe, *Citrus sinensis* fruit peel methanol extract; DWP, dry weight peel; FBG, fasting blood glucose; HDL-c, high-density lipoprotein cholesterol; HOMA-IR, homeostasis model assessment of insulin resistance; HRP, horseradish peroxidase; ITT, insulin tolerance test; LDL-c, low-density lipoprotein cholesterol; OGTT, oral glucose tolerance test; PBS, phosphate-buffered saline; PBST, phosphate-buffered saline-Tween 20; RSD, relative standard deviation; SEM, standard error of the mean; SGOT, serum glutamic oxaloacetic transaminase; SGPT, serum glutamic pyruvic transaminase; STZ, streptozotocin; T2DM, type 2 diabetes mellitus; TC, total cholesterol; TG, triglycerides.

ABSTRACT

Citrus sinensis (L.) Osbeck is extensively cultivated worldwide and one of the most consumed fruits in the world. We evaluated the therapeutic properties of the methanol extract from *Citrus sinensis* fruit peel (CSMe) in high-fat diet-fed streptozotocin-induced insulin-resistant diabetic rats. Body weight, food intake, and water consumption were analysed. Biochemical and molecular biologic indices, and the expression of insulin receptor-induced signalling molecules were assessed to identify possible mechanisms. In addition, we conducted histology of pancreatic and adipose tissues. UHPLC-MS/MS analysis showed the presence of 17 dietary phenolics at substantial concentrations. High-fat diet-fed streptozotocin-induced diabetic rats administered CSMe (50 and 100 mg/kg) had reduced fasting blood glucose (56.1% and 55. 7%, respectively) and plasma insulin levels (22.9% and 32.7%, respectively) compared with untreated diabetic control rats. CSMe reversed the biochemical abnormalities in diabetic rats, showed cytoprotective activity, and increased the intensity of the positive immunoreactions for insulin in pancreatic islets. CSMe treatment increased the expression of PPARγ in the adipose tissue and signalling molecules GLUT4 and insulin receptor. Our data suggest that CSMe could optimize glucose uptake of adipose tissues through the insulin-dependent signalling cascade mechanism and it should be investigated in the management of individuals with type 2 diabetes mellitus.

Keywords: Adipose; *Citrus sinensis*; Diabetes; Histology; Insulin receptor; Pancreatic β-cell

1. Introduction

Type 2 diabetes mellitus (T2DM) is one of the most prevalence chronic diseases resulting in severe complications, such as nephropathy, neuropathy, retinopathy, cardiovascular morbidity and premature mortality (Dewanjee et al., 2009). Its relenting increase worldwide imposes a huge financial burden on healthcare systems (Seuring et al., 2015). T2DM is characterised by pancreatic β-cell dysfunction, hyperglycaemia, and dyslipidaemia that result from metabolic deregulations, inappropriate glucose utilization and distortion of the insulin signalling pathway (Sharma et al., 2008). Natural products are a common source of new chemical or therapeutic molecules for T2DM (Newman and Cragg, 2012; 2016). Many plants are used in ethnopharmacology to treat symptoms of T2DM, including several polyphenolic compounds such as fukugetin, palmatine, berberine and others (Rios et al., 2015; Gushiken et al., 2016). Moreover, many natural products can stimulate insulin signalling with possible applicability to T2DM, resulting in a growing number of patents (Singh and Mahajan, 2013; Salimifar et al., 2013; Tamrakar et al., 2014).

Citrus sinensis (L.) Osbeck (Rutaceae), commonly known as the sweet orange, is ubiquitous in human diet across the world (Lv et al., 2015) and belongs to the citrus family (Duarte et al., 2016). *C. sinensis* peel is a rich source of phenolic compounds, with antidiabetic, antioxidant, and free radical scavenging activities, effects against gastrointestinal illnesses, and potential protection against different cancers and cardiovascular disorders (Rotelli et al., 2003; Selmi et al., 2017). A number of recent experiments have explored the therapeutic potential of phenolics derived from citrus species as a single bioactive molecule (Selmi et al., 2017). *C. sinensis* peel exhibits hypoglycaemic and hypolipidaemic effects in an alloxan-induced animal model of type 1 diabetes (Luka et al., 2017). However, no comprehensive studies have explored the therapeutic potential of the standardised extract of *C. sinensis* peel in high-fat diet-fed rats with streptozotocin (STZ)-

induced type 2 diabetes. Therefore, the present investigation was designed to analyse the phenolic composition and antidiabetic effect of *C. sinensis* peel and evaluate its effects on insulin receptor-induced signalling in a rat model of obesity and T2DM.

2. Material and methods

2.1. Chemicals and reagents

Methanol and acetonitrile were purchased from Merck (New Jersey, USA). The water used for the mobile phase was purified by using a Milli-Q system (*Direct-Q*® 3UV, Millipore, São Paulo, Brazil). STZ, apigenin, artepillin C, cinnamic acid, caffeic acid, ferulic acid, caffeic acid phenyl ester (CAPE), (+)-catechin, ethyl gallate, kaempferide, acacetin, naringenin, *p*-coumaric acid, protocatechuic acid, chrologenic acid, rutin, vanillin, vanillic acid, and all other high-purity chemicals were acquired from Sigma-Aldrich (St Louis, MO, USA). Nylon membranes (47 mm i.d. × 0.45 µm) were used to filter the samples and were purchased from São Paulo, Brazil.

2.2. Fruit material

Fresh *C. sinensis* fruits were collected from agricultural fields of the municipality of Cristinápolis, in Sergipe state, Brazil in February 2016 and were authenticated by the botanist of the Federal University of Sergipe. The fruits were washed with distilled water and peeled. The *C. sinensis* peels were dried at 40ºC, grounded in a food processor, and immediately subjected to the extract preparation process.

2.3. Extract preparation

C. sinensis peels were processed as described by Mishra et al. (2012). 100 mg of fruit peel powder were added to methanol (150 mL) and heated at 55°C for 5 min. The solution was sealed with a glass stopper and kept on the rotary shaker for 24 h. Finally, the solvent was evaporated at 45°C using a rotary evaporator, the extract was reconstituted at 50 mg/mL in

methanol and filtered through a membrane filter (0.45 µm). The residues were further dried in an oven at 30°C to remove traces of the solvent and stored in an airtight glass container at 4-5°C until use. After solvent evaporation, the percentage yield of the methanol extract obtained from the orange peel was 5.18% (w/w). The extract was dissolved in vehicle containing 0.2% polysorbate-80, 0.5% sodium carboxymethyl cellulose, 0.9% sodium chloride, 0.9% benzyl alcohol, and 97.5% distilled water (Lee, 2001) and then used for experimentation.

2.4. UHPLC-MS/MS conditions

The identification and quantification of phenolic compounds present in *C. sinensis* peels was conducted as described by Andrade et al. (2017). The phenolic profile analysis was performed by using a UHPLC system model 1290 Infinity coupled to a 6490 TripleQuad mass spectrometer equipped an electrospray ionization system (Agilent Technologies, Palo Alto, USA). The chromatographic separations were performed on an Ascentis Express F5 column, 2.7 µm particle size and 150 × 2.1 mm i.d. (Sigma Aldrich). The mobile phase consisted of 0.1% (v/v) aqueous formic acid solution (A) and acetonitrile (B), with a flow rate of 0.2 mL/min, eluted with the following gradient profile at 40°C: 0-1 min, 15% B; 1-7 min, 25% B; 7-9 min, 25% B; 9-13 min, 30% B; 13-16 min, 30% B; 16-21 min, 40% B; 21-23 min, 40% B; 23-25 min, 45% B; 25-28 min, 50% B; 28-33 min, 60% B; 33-37 min, 75% B; and 37-38 min, 15% B. The injection volume was 2 µL. The LC-MS data were acquired by using the MassHunter software. A standard calibration curve was prepared from eight data points in the concentration range of 20-1000 ng/mL. All analyses were performed in triplicate. The precision of the replicates was expressed by their relative standard deviation (RSD).

The mass spectrometry conditions were: source temperature, 200ºC; gas flow, 12 L/h; nebuliser, 20 psi; sheath gas temperature, 400°C; sheath gas flow, 11 L/min; capillary voltage, 3500 V; nozzle voltage, 500 V; acceleration cell voltage, 5 V; and dwell time, 9.8

ms. To obtain the maximum sensitivity for the identification and detection of all target compounds, two selected reaction monitoring transitions were monitored for each compound. The electrospray ionization source was operated in positive mode, except for CAPE, for which a negative mode was used.

2.5. Experimental animals

All animal procedures were approved in accordance with the Institutional Ethical Committee for the use and care of experimentation on animals based on US National Institutes of Health Publication. Healthy male Wistar rats (weight: 180-200 g) were housed in polypropylene cages, fed a standard chow diet (10% energy from fat, 76% from carbohydrates, and 14% from proteins; 3.8 kcal/g), and provided tap water *ad libitum*. The animals were maintained and acclimatised under controlled conditions (temperature, 22°C ± 2°C; relative humidity, 60% ± 5%) with a 12:12 h light/dark cycle for 7 days after arrival.

2.6. Acute oral toxicity study

Healthy male rats (weight: 180-200 g) were fasted overnight with no prior drug treatments and divided equally into three groups of six rats each. CSMe was administered orally at 0.5 and 1 g/kg concentrations, suspended in a vehicle containing 0.2% polysorbate-80, 0.5% sodium carboxymethyl cellulose, 0.9% sodium chloride, 0.9% benzyl alcohol, and 97.5% distilled water (3 mL/100 g) for the treatment groups. The control group was administered the vehicle (3 mL/100 g) alone. The rats were allowed free access to food and water from 4 h after the CSMe administration. All the animals were closely observed for the initial 4 h and then every day over a period of 14 days for signs of mortality, drowsiness, restlessness, writhing, convulsions, piloerection; analysis of urine and faeces. The animals were sacrificed on day 15 and the vital organs were observed for gross pathological lesions. CSMe (0.5 and 1 g/kg) did not result in any deaths, although mild physiological alterations were observed at 1

g/kg. No treatment-associated gross pathological alterations were witnessed. Hence, doses of 50 and 100 mg were selected for subsequent experiments, based on the results of Oliveira et al. (2008).

2.7. Development of the T2DM model

T2DM was induced in experimental rats by feeding a standardised high-fat diet (55% energy from fat, 31% from carbohydrates, and 14% from proteins; 5.9 kcal/g) for 2 weeks prior to a single intraperitoneal injection of STZ (40 mg/kg) dissolved in 0.1 M citrate buffer (pH 4.5). The rats received tap water and the high-fat diet throughout the study. Initial drug-induced hypoglycaemic mortality was avoided in STZ-injected rats by the administration of a 20% glucose solution for 24 h. The rats in the non-diabetic control group were injected with the citrate buffer solution and received tap water and the commercial chow diet during the experiment. Blood samples were collected from the tail vein after 5 days of STZ induction; hyperglycaemia was evaluated through the measurement of fasting blood glucose (FBG) levels (Trinder, 1969). Rats with FBG > 250 mg/dL were classified as diabetic and used in the study. Subsequently, the experiment commenced on day 0 (3 days after the induction of diabetes) and the high-fat diet was maintained throughout the study.

2.8. Experimental design

Twenty four diabetic and 6 normal rats were randomly divided into five groups, containing six rats each, and administered the following treatments:

Group I: Normal control rats received vehicle 1 mL/100 g

Group II: Diabetic control rats received vehicle 1 mL/100 g

Group III: Diabetic rats treated with CSMe 50 mg/kg suspended in vehicle (1 mL/100 g)

Group IV: Diabetic rats treated with CSMe 100 mg/kg suspended in vehicle (1 mL/100 g)

Group V: Diabetic rats treated with metformin 100 mg/kg suspended in vehicle (1 mL/100 g)

The vehicle or test drugs were administered by gavage between 12.00 and 2.00 p.m, once a day, for 30 days.

2.9. Biochemical analysis

The intake of food and water was estimated once per day during the experiment. FBG and body weight were measured on days 0, 14, 21, and 28. Plasma insulin, determined by an ultrasensitive rat insulin ELISA kit, total cholesterol (TC), triglycerides (TG), high (HDL-c), and low-density lipoprotein cholesterol (LDL-c) were determined on days 0 and 28**.** The Homeostasis Model Assessment of insulin resistance (HOMA-IR) was calculated as described by Matthews et al. (1985). An oral glucose tolerance test (OGTT) was conducted on day 15. Briefly, the rats were fasted for 6 h and, a glucose solution (2 g/kg) was orally administered to each rat 30 min after the administration of the extract, standard drug, or vehicle. The blood glucose was analysed at time 0 (prior to the glucose administration) and at 30, 60, and 120 min after the glucose infusion. On day 25, an insulin tolerance test (ITT) was conducted. Briefly, after fasting for 6 h, blood samples were collected from the tail vein into heparin-coated tubes. The animals were intraperitoneally administered a dose of 1.2 U/kg insulin (*Huminsulin R;* Eli Lilly) in normal saline. Blood samples were then collected 30 and 60 min after the insulin injection, from which the glucose level was estimated. On day 30, the animals were anaesthetised and sacrificed by cervical decapitation in accordance with animal ethics guidelines. The blood was collected in a dry test tube and allowed to coagulate at room temperature for 30 min. The serum was then separated by centrifugation at 2000 rpm for 10 min and serum glutamic oxaloacetic transaminase (SGOT) and serum glutamic pyruvic transaminase (SGPT) were estimated using Reitman and Frankel method (1957). The activity of serum alkaline phosphatase (ALP) was determined using the method of Kind and King

(1954). Serum urea and creatinine were measured by using the diacetyl monoxime method (Wybenga et al., 1971) and Jaffe's method (Slot, 1965), respectively.

2.10. Histology

The histology of pancreas and adipose was examined in accordance with previously described protocols (Gandhi et al., 2012).

2.11. Immunohistochemical analysis

Pancreatic tissues were fixed in 10% neutral buffered saline, embedded in paraffin, and prepared as 5 µm thick sections. The tissues were fixed on a clean microscope slide and deparaffinised in a xylene bath. The slides were dehydrated with two rinses in absolute alcohol and two rinses in 95% ethanol for 3 min each. The tissue sections were placed in 0.3% hydrogen peroxide (2 mL H_2O_2 in 18 mL methanol) and 5% normal bovine serum (1:5 diluted PBS) for 20 min at room temperature, respectively, to block the endogenous peroxidase and non-specific binding sites for antibodies. To detect insulin, the sections were incubated with polyclonal guinea-pig anti-insulin (1:250 dilution) and horseradish peroxidase (HRP)-conjugated streptavidin for 30 min, respectively. The sections were washed in PBS and incubated with biotinylated anti-mouse IgG (1:500 dilution). After incubation for 30 min, the sections were washed again with PBS and excess buffer was removed from the slides, which were then incubated with diaminobenzidine for 3-5 min at room temperature and then washed with distilled water. Finally, the slides were stained with haematoxylin, dehydrated, and mounted in glycerin-gelatin (Gandhi et al., 2011). The results were scored through multiplication of the percentage of positive cells (P) with the intensity of staining (I). Formula: Score = P × I (McDonald and Pilgram, 1999).

2.12. RNA extraction and reverse transcriptase-polymerase chain reaction (RT-PCR) analysis

RT-PCR was performed as described by Lee et al. (2010). Total RNA was isolated from adipose tissue by using TRIzol reagent in accordance with the manufacturer's instructions and reverse-transcribed into cDNA. The following gene-specific primers were used: PPARγ, 5'-TCAGGGCTGCCAGTTTCG-3' (forward), 5'-GCTTTTGGCATACTCTGTGATCTC-3' (reverse); GLUT4, 5'-GACATTTGGCGGAGCCTAAC-3' (forward), 5'-TAACTCCAGCAGGGTGACACAG-3' (reverse); insulin receptor (IR), 5'-TGACAATGAGGAATGTGGGGAC-3' (forward), 5'-GGGCAAACTTTCTGACAATGACTG-3' (reverse); β-actin, 5'-TGTTGTCCCTGTATGCCTCT-3' (forward), 5'-TAATGTCACGCACGATTTCC-3' (reverse). The reaction mixtures were resolved on 2% agarose gels, stained with ethidium bromide, and photographed.

2.13. Western blot analysis

Total protein (100 µg) extracted from the adipose tissue of the experimental rats was suspended in substrate-soluble buffer and resolved by 10% SDS-PAGE. Subsequently, the proteins were transferred to a nitrocellulose membrane, which was blocked with 5% non-fat dry milk at 4°C for 1 h and probed overnight with primary antibodies for PPARγ, GLUT4, IR, and β-actin (which were diluted to 1:1000). After three washes for 5 min each in PBS-Tween 20 (PBST), the membranes were incubated with HRP-conjugated rabbit-anti mouse or goat-anti rabbit secondary antibodies (which were diluted to 1:5000) for 1 h. The obtained blots were further washed three times with PBST and the protein band was detected using an enhanced chemiluminescence detection system (Mullainadhan et al., 2017).

2.14. Statistical analysis

The results are expressed as the mean ± standard error of the mean (SEM). The statistical significance was evaluated by one-way analysis of variance followed by Dunnett's C post-

hoc test computed by using SPSS 11.5 for Windows. Differences with a *P* value of < 0.05 were considered significant.

3. Results

3.1. Quantification of phenolic compounds in CSMe by UHPLC-MS/MS

To validate the UHPLC-MS/MS method, calibration curves were run between sample analyses. The linearity parameters of method verification are presented in Table 1. The external calibration curves were constructed for each standard by plotting the peak area versus the nominal concentration. The method verification was in accordance with the analytical method validation guidelines (US-FDA, 2000) with regression analysis (r^2) values above 0.99 (Table 1). The individual compounds were quantified from the ratio of the peak areas of the identified compounds relative to the peak areas of the corresponding analytical standard. The quantification of the phenol compounds in CSMe are detailed in Table 2 and their chemical structures are shown in Figures 2 and 3. The chromatographic profile of CSMe is shown in Figure 1A. Seventeen phenolic compounds were identified and quantified in CSMe by UHPLC-MS/MS. The target compounds were identified by monitoring of the specific fragmentations of each analytical standard and their corresponding retention times. The compounds rutin (1248.3 µg/g), *p*-coumaric acid (957.4 µg/g), protocatechuic acid (326.3 µg/g), ferulic acid (316.0 µg/g), and naringenin (220.7 µg/g) of dry weight peel (DWP) were the major constituents of CSMe.

3.2. Effect of CSMe on the intake of food and water in high-fat diet-fed STZ-induced diabetic rats

High-fat diet-fed STZ-induced diabetic rats exhibited a significant increase in food and water consumption compared with normal control rats at the start of the intervention. The

treatment with CSMe (50 and 100 mg/kg) significantly reduced food and water intake compared with diabetic control rats by the end of the study (Table 3).

3.3. Effect of CSMe on OGTT and ITT parameters

The oral administration of glucose gradually increased the blood glucose level in all groups at 30 min, which remained unchanged over the next 120 min in the diabetic control rats. In diabetic rats receiving CSMe (50 and 100 mg/kg) or metformin, the blood glucose levels decreased at 60, and 120 min after glucose administration, although they remained significantly higher than the normal controls at 120 min (Table 4). CSMe (50 and 100 mg/kg) treated diabetic rats also had significant clearance of blood glucose over the experimental period of the ITT compared with diabetic control rats and reached similar blood glucose levels as metformin after 60 min (Table 5).

3.4. Effect of CSMe on FBG and body weight

The FBG levels and body weight of control and experimental rats at 0, 14, 21, and 28 days of treatment are shown in Tables 6 and 7. CSMe (50 and 100 mg/kg) and metformin treated rats significantly decreased FBG levels by 56.1%, 55.6% and 55.7% respectively, after 28 days of treatment compared with the diabetic control rats. Body weight gain was significantly higher in high-fat diet-fed STZ-induced diabetic rats than in normal control rats during the experimental period. CSMe (50 and 100 mg/kg) treatment resulted in a smaller body weight gain in diabetic rats compared with diabetic control rats, but these differences were not statistically significant.

3.5. Effect of CSMe on plasma insulin and HOMA-IR

High-fat diet-fed STZ-induced diabetic rats had a significant increase in plasma insulin levels and HOMA-IR compared with normal control rats (day 0 of Table 8). CSMe (50 and 100 mg/kg) and metformin treatment resulted in a significant decrease in the plasma insulin

levels (22.9% and 32.7% and 23.2%, respectively) in the diabetic rats. CSMe and metformin also decreased the HOMA-IR during the follow up study period (day 28, Table 8).

3.6. Effect of CSMe on TC, TG, LDL-c, and HDL-c

The TC, TG, and LDL-c levels were significantly higher in diabetic control rats than in the normal control group. In contrast, HDL-c levels were lower in the diabetic control group than in the normal control group. CSMe (50 and 100 mg/kg) and metformin significantly reduced the levels of TC, TG, and LDL-c and significantly improved the level of HDL-c compared with the diabetic control rats (Figure 4).

3.7. Effect of CSMe on SGOT, SGPT, ALP, urea, and creatinine

The activity and levels of SGOT, SGPT, ALP, urea, and creatinine were significantly higher in diabetic control rats than in normal control rats, as shown in figure 5. The administration of CSMe (50 and 100 mg/kg) or metformin for 30 days significantly restored the activities of SGOT, SGPT, and ALP, and increased the levels of urea and creatinine, with the reductions being more marked with CSMe at 100 mg/kg and metformin.

3.8. Histology and immunohistochemical analysis

Histological results are shown in Figures 6 and 7. The pancreatic tissue of diabetic rats had degranulated β-cells and widespread vacuolisation with disordered islet architecture. High-fat diet-fed STZ-induced diabetic rats exhibited a swollen arrangement of cells in the epididymal adipose tissue. In contrast, the tissues in CSMe-treated diabetic rats showed normal distributions with apparently regular architecture in adipose tissue and pancreatic islets. The immunohistochemical analysis of pancreatic islets is shown in Figure 8. Diabetic control rats showed a significant decrease in the intensity of positive staining for insulin compared with normal control rats. In contrast, the rats receiving CSMe had a significant increase in the intensity of insulin staining compared with diabetic control rats. The

immunostaining of insulin in the β-cells of the islet tissues is shown in Figure 9. Diabetic control rats had a significant reduction in the level of insulin immunostaining expression compared with control rats. Conversely, CSMe-treated rats exhibited a significant increase in insulin expression compared with the diabetic control group.

3.9. Effect of CSMe on expression on PPARγ, GLUT4, and IR in adipose tissue

PPARγ, GLUT4, and IR mRNA expression levels in CSMe-treated diabetic groups were significantly higher than those in the diabetic control group (Fig. 10A). Similar changes were observed in the protein expression of PPARγ, GLUT4, and IR (Fig. 10B).

4. Discussion

T2DM is projected to be one of the major causes of morbidity and mortality in the 21st century and novel compounds to improve the metabolism of glucose and the long term deleterious effects of diabetes are needed (Jaacks et al., 2016). Earlier studies have demonstrated that a combined high-fat diet and a low-dose STZ (40 mg/kg) results in insulin-resistance in rats, with elevation of plasma lipids (Srinivasan et al., 2005). The high-fat diet induces insulin resistance through accumulation of lipids, including free fatty acids, their COA esters, and triglycerides in adipose tissues, skeletal muscle, and the liver of experimental animals, as well as an oxidative imbalance caused by oxidative stress (Krol and Krejpcio, 2011; Veerapur et al., 2012). Low-dose STZ results in the partial destruction of β-cells, which may be responsible for the long-term glycaemic imbalance in rats (Zhang et al., 2010). Polyphenols of plant origin may have pharmacological properties, as adjuvants for the management of symptoms and biomarkers of patients with T2DM (Bahadoran et al., 2013).

In the present study, a methanolic orange peel extract, which is rich in polyphenols, resulted in significant glucose-lowering effects in diabetic rats compared with a diabetic control group when challenged in a OGTT and ITT experiments. These results were similar

to those elicited by metformin, which is one of the most commonly used drugs for diabetes management. CSMe may have increased the glucose uptake by improving insulin sensitivity through a glucose-utilising effect in the peripheral tissues. CSMe significantly restored the insulin levels and HOMA-IR compared with the diabetic control rats, which signifies that its insulin-sensitising effects may be associated through a decrease in insulin resistance.

As expected, STZ-induced diabetic rats receiving a high-fat diet had significant hyperglycaemia compared with normal control rats. CSMe significantly reduced the FBG level in diabetic rats by improving the physiological functions of PPARγ in adipose tissue. CSMe upregulated the expression levels of PPARγ, GLUT4, and IR in the adipose tissues of diabetic rats. These findings showed that CSMe-mediated PPARγ activation stimulated adipocyte differentiation and enhanced IR signalling via the translocation and activation of GLUT4 in PI3K/p-Akt pathway in the adipose tissue. These results corroborate similar findings by Mohammadi et al. 2014. Indeed, *Zataria multiflora,* a plant containing extensive phenol compounds was determined to be a PPARγ agonist, improving insulin-sensitizing activity and increase in translocation and activation of GLUT4 in high fructose fed insulin resistant rats.

The UHPLC-MS/MS also showed that CSMe contains major polyphenol components such as rutin, *p*-coumaric acid, protocatechuic acid, ferulic acid, and naringenin, which, in total, comprised 3.7438 mg of the dry weight peel in addition to other minor biophenolics, such as apigenin, artepillin C, cinnamic acid, caffeic acid, CAPE, (+)-catechin, ethyl gallate, kaempferide, chrologenic acid, acacetin, vanillin, and vanillic acid. It is thus likely, a combination of these compounds could be responsible for the antidiabetic activity of CSMe. Our results are in agreement with an earlier report that described the synergistic hypoglycaemic and insulin-sensitising effect of phenolic constituents derived from *Aristotelia chilensis* in T2DM mice (Rojo et al., 2012). Although the overall mechanism of the CSMe-

mediated reversal of hyperglycaemia has not been elucidated, our findings may suggest the phenolic constituents exert potent synergistic action on the PPARγ receptor, stimulate GLUT4 translocation and activate via an insulin-dependent pathway in adipose tissue, and reduce glucose levels in blood.

Our results demonstrated that the combination of a high-fat diet and STZ markedly increased the levels of TC, TG, LDL-c, and decreased that of HDL-c. Hyperlipidaemia is a crucial factor in the pathophysiology of T2DM, which is responsible for severe diabetic complications (Verges, 2015). The increased TG levels and decreased HDL-c levels in diabetic rats may result from their larger high-fat diet intake. The enlargement of epidydimal adipose cells and increase in body weight gain were also observed in the high-fat diet fed diabetic rats. The administration of CSMe to diabetic rats markedly improved the lipid profile, the altered glycaemia and the morphological variations in adipose tissue. These observations are in agreement with Sharma et al. (2015) who reported that phenolic-rich extracts of *Brassica oleracea var gongylodes* act as a multi-component extract therapy that exhibits a marked control on the lipid profile and blood glucose levels. The findings of the study also demonstrated that the extract affected the antioxidative capacity in the diabetic condition.

The increase in SGOT, SGPT, and ALP might reflect the outflow of these enzymes from the liver cytosol into the blood stream (Navarro et al., 1993). CSMe treatment decreased these enzymes levels compared with the diabetic control group and alleviated the liver injury caused by high-fat diet fed STZ. In diabetic rats, increased levels of urea and creatinine were observed in the serum (Bethesda, 2001) and diabetic rats treated with CSMe exhibited a reduction in serum urea and creatinine. The depletion of renal status in diabetic rats was caused by the production of reactive oxygen species as an outcome of the elevated free radical concentration in these tissues (Fakhruddin et al., 2017). CSMe restored the renal

condition in treated diabetic rats, possibly through the neutralisation of free radicals. Gandhi et al. (2014) reported that high-fat diet fed STZ-induced diabetes disrupts the function of β-cells in experimental rats and we found marked degranulation, decreased β-cell mass, and reduced insulin expression in the diabetic control group. The oral supplementation of CSMe preserved β-cell integrity and increased insulin expression, thus implying that CSMe exerted a cytoprotective effect with the reversal of β-cell damage caused by STZ.

5. Conclusion

The present study suggests that phenolic-rich CSMe confers an insulin-sensitising effect on high-fat diet-fed STZ-induced diabetic rats, which improved the upregulation of PPARγ, GLUT4, and IR in the adipose tissue. CSMe has therapeutic potential against dyslipidaemia; which may be accompanied by protective effects on the structure and function of β-cell.

Declaration of Conflict of Interest

The authors declare that there are no conflicts of interest.

Acknowledgement

GRG thanks the Programa Nacional de Pós-Doutorado da Coordenação de Aperfeiçoamento de Pessoal de Nível Superior (PNPD/CAPES) for assistance in the form of a Postdoctoral Internship (Process Number: 1666288). GRG, JSSQ, LJQJ and RQG are researchers of the Post-Graduation Program in Health Sciences of the Federal University of Sergipe (Brazil).

References

Andrade, J.K.S., Denadai, M., de Oliveira, C.S., Nunes, M.L., Narain, N., 2017. Evaluation of bioactive compounds potential and antioxidant activity of brown, green and red propolis from Brazilian northeast region. Food Res. Int. 101, 129-138.

Bahadoran, Z., Mirmiran, P., Azizi, F., 2013. Dietary polyphenols as potential nutraceuticals in management of diabetes: a review. J. Diabetes Metab. Disord. 12, 43.

Bethesda, M.D., 2001. US Renal Data System. Annual Data Report: Atlas of End Stage Renal Disease in the United States: National Institutes of Health. National Institute of Diabetes and Digestive and Kidney Diseases.

Dewanjee, S., Das, A.K., Sahu, R., Gangopadhyay, M., 2009. Antidiabetic activity of *Diospyros peregrina* fruit: effect on hyperglycemia, hyperlipidemia and augmented oxidative stress in experimental type 2 diabetes. Food Chem. Toxicol. 47, 2679–2685.

Duarte, A., Fernandes, J., Bernardes, J., Miguel, G., 2016. Citrus as a component of the Mediterranean diet. J. Spat. Org. Dyn. 4, 289–304.

Fakhruddin, S., Alanazi, W., Jackson, K.E., 2017. Diabetes-induced reactive oxygen species: mechanism of their generation and role in renal injury. J. Diabetes Res. 2017, 1–30.

Gandhi, G.R., Ignacimuthu, S., Paulraj, M.G., 2011. *Solanum torvum* Swartz. fruit containing phenolic compounds shows antidiabetic and antioxidant effects in streptozotocin induced diabetic rats. Food. Chem. Toxicol. 49, 2725–2733.

Gandhi, G.R., Ignacimuthu, S., Paulraj, M.G., 2012. Hypoglycemic and β-cells regenerative effects of *Aegle marmelos* (L.) Corr. bark extract in streptozotocin-induced diabetic rats. Food Chem. Toxicol. 50, 1667–1674.

Gandhi, G.R., Vanlalhruaia, P., Stalin, A., Irudayaraj, S.S., Ignacimuthu, S., Paulraj, M.G., 2014. Polyphenols-rich *Cyamopsis tetragonoloba* (L.) Taub. beans show

hypoglycemic and β-cells protective effects in type 2 diabetic rats. Food Chem. Toxicol. 66, 358–365.

Gushiken, L.F., Beserra, F.P., Rozza, A.L., Bérgamo, P.L., Bérgamo, D.A., Pellizzon, C.H., 2016. Chemical and biological aspects of extracts from medicinal plants with antidiabetic effects. Rev. Diabet. Stud. 13, 96-112.

Jaacks, L.M., Siegel, K.R., Gujral, U.P., Narayan, K.M., 2016. Type 2 diabetes: A 21st century epidemic. Best Pract. Res. Clin. Endocrinol. Metab. 30, 331-343.

Kind, P.R.N., King, E.J., 1954. Estimation of plasma phosphatases by determination of hydrolyzed phenol with amino-antipyrine. J. Clin. Pathol. 7, 322–330.

Krol, E., Krejpcio, Z., 2011. Evaluation of anti-diabetic potential of chromium (III) propionate complex in high-fat diet fed and STZ injected rats. Food Chem. Toxicol. 49, 3217–3223.

Lee, K.M., 2001. Overview of drug product development. Curr. Protoc. Pharmacol. 7, 1–10.

Lee, Y.S., Cha, B.Y., Saito, K., Yamakawa, H., Choi, S.S., Yamaguchi, K., Yonezawa, T., Teruya, T., Nagai, K., Woo, J.T., 2010. Nobiletin improves hyperglycemia and insulin resistance in obese diabetic *ob/ob* mice. Biochem. Pharmacol. 79, 1674–1683.

Luka, C.D., Istifanus, G., George, M., Philip, C.J., 2017. The effect of aqueous extract of *Citrus sinensis* peel on some biochemical parameters in normal and alloxan-induced diabetic wister rats. Am. J. Phyto. Clin. Therap. 5, 17.

Lv, X., Zhao, S., Ning, Z., Zeng, H., Shu, Y., Tao, O., Xiao, C., Lu, C., Liu, Y., 2015. Citrus fruits as a treasure trove of active natural metabolites that potentially provide benefits for human health. Chem. Cent. J. 9, 68.

Matthews, D.R., Hosker, J.P., Rudenski, A.S., Naylor, B.A., Treacher, D.F., Turner, R.C., 1985. Homeostasis model assessment: insulin resistance and beta-cell function from fasting plasma glucose and insulin concentrations in man. Diabetologia 28, 412–419.

McDonald, J.W., Pilgram, T.K., 1999. Nuclear expression of p53, p21 and cyclin D1 is increased in bronchioloalveolar carcinoma. Histopathology 34, 439–446.

Mishra, G.J., Reddy, M.N., Rana, J.S., 2012. Isolation of flavonoid constituent from *Launaea procumbens* Roxb. by preparative HPTLC Method. IOSR J. Pharm. 2, 5–11.

Mohammadi, A., Gholamhoseinian, A., Fallah, H., 2014. *Zataria multiflora* increases insulin sensitivity and PPARγ gene expression in high fructose fed insulin resistant rats. Iran J. Basic Med. Sci. 17, 263-270.

Mullainadhan, V., Viswanathan, M.P., Karundevi, B., 2017. Effect of Bisphenol-A (BPA) on insulin signal transduction and GLUT4 translocation in gastrocnemius muscle of adult male albino rat. Int. J. Biochem. Cell Biol. 90, 38-47.

Navarro, M.C., Montilla, M.P., Martin, A., Jimenez, J., Utrilla, M.P., 1993. Free radicals scavenger and antihepatotoxic activity of *Rosmarinus tomentosus*. Plant Med. 59, 312–314.

Newman, D.J., Cragg, G.M., 2012. Natural products as sources of new drugs over the 30 years from 1981 to 2010. J. Nat. Prod. 75, 311-335.

Newman, D.J., Cragg, G.M., 2016. Natural products as sources of new drugs from 1981 to 2014. J. Nat. Prod. 79, 629-661.

Oliveira, H.C., Santos, M.P.D., Grigulo, R., Lima, L.L., Martins, D.T., Lima, J.C., Stoppiglia, L.F., Lopes, C.F., Kawashita, N.H., 2008. Antidiabetic activity of *Vatairea macrocarpa* extract in rats. J. Ethnopharmacol. 115, 515–519.

Reitman, S., Frankel, S.A., 1957. Colorimetric method for the determination of serum glutamic oxaloacetic and glutamic pyruvic transaminases. Am. J. Clin. Pathol. 28, 56–63.

Ríos, J.L., Francini, F., Schinella, G.R., 2015. Natural products for the treatment of type 2 diabetes mellitus. Planta Med. 81, 975-994.

Rojo, L.E., Ribnicky, D., Logendra, S., Poulev, A., Rojas-Silva, P., Kuhn, P., Dorn, R., Grace, M.H., Lila, M.A., Raskin, I., 2012. *In vitro* and *in vivo* anti-diabetic effects of anthocyanins from Maqui Berry (*Aristotelia chilensis*). Food Chem. 131, 387–396.

Rotelli, A.E., Guardia, T., Juárez, A.O., De, L., Pelzer, L.E., 2003. Comparative study of flavonoids in experimental models of inflammation. Pharmacol. Res. 48, 601-606.

Salimifar, M., Fatehi-Hassanabad, Z., Fatehi, M., 2013. A review on natural products for controlling type 2 diabetes with an emphasis on their mechanisms of actions. Curr. Diabetes Rev. 9, 402-411.

Selmi, S., Rtibi, K., Grami, D., Sebai, H., Marzouki. L., 2017. Protective effects of orange (*Citrus sinensis L.)* peel aqueous extract and hesperidin on oxidative stress and peptic ulcer induced by alcohol in rat. Lipids Health Dis. 16, 152.

Seuring, T., Archangelidi, O., Suhrcke, M., 2015. The economic costs of type 2 diabetes: A global systematic review. PharmacoEconomics 33, 811-831.

Sharma, B., Balomajumder, C., Roy, P., 2008. Hypoglycemic and hypolipidemic effects of flavonoid rich extract from *Eugenia jambolana* seeds on streptozotocin induced diabetic rats. Food Chem. Toxicol. 46, 2376–2383.

Sharma, I., Aaradhya, M., Kodikonda, M., Naik, P.R., 2015. Antihyperglycemic, antihyperlipidemic and antioxidant activity of phenolic rich extract of *Brassica oleraceae var gongylodes* on streptozotocin induced Wistar rats. Springerplus 4, 212.

Singh, P., Mahajan, S., 2013. Berberine and its derivatives: a patent review (2009-2012). Expert Opin. Ther. Pat. 23, 215-231.

Slot, C., 1965. Plasma creatinine determination: A new and specific Jaffe reaction method. Scand J. Clin. Lab. Invest. 17, 381–387.

Srinivasan, K., Viswanad, B., Asrat, L., Kaul, C.L., Ramarao, P., 2005. Combination of high-fat diet-fed and low-dose streptozotocin-treated rat: a model for type 2 diabetes and pharmacological screening. Pharmacol. Res. 52, 313–320.

Tamrakar, A.K., Maurya, C.K., Rai, A.K., 2014. PTP1B inhibitors for type 2 diabetes treatment: a patent review (2011 - 2014). Expert Opin. Ther. Pat. 24, 1101-1115.

Trinder, P., 1969. Determination of glucose in blood using glucose oxidase with an alternative oxygen acceptor. Ann. Clin. Biochem. 6, 24–27.

US-FDA., 2000. United States Food and Drug Administration-Guidance for Industry, Bioanalytical Method Validation.

Veerapur, V.P., Prabhakar, K.R., Thippeswamy, B.S., Bansal, P., Srinivasan, K.K., Unnikrishnan, M.K., 2012. Antidiabetic effect of *Ficus racemosa* Linn. stem bark in high-fat diet and low-dose streptozotocin-induced type 2 diabetic rats: a mechanistic study. Food Chem. 132, 186–193.

Verges, B., 2015. Pathophysiology of diabetic dyslipidaemia: where are we? Diabetologia 58, 886–899.

Wybenga, D.R., Di-Giorgio, J., Pileggi, V.J., 1971. Manual and automated methods for urea nitrogen measurement in whole serum. Clin. Chem. 17, 891-895.

Zhang, L., Yang, J., Chen, X.Q., Zan, K., Wen, X.D., Chen, H., Wang, Q., Lai, M.X., 2010. Antidiabetic and antioxidant effects of extracts from *Potentilla discolor* Bunge on diabetic rats induced by high fat diet and streptozotocin. J. Ethnopharmacol. 132, 518-524.

Table 1: Method verification linearity

Phenolic	Equation	r^2	Retention time (min)
Acacetin	y = 6587 + 69212 x	0.998	24.2
Apigenin	y = 11116 + 2146 x – 0.4294 x^2	0.999	17.7
Artepillin C	y = 12979 +1680 x + 0.7351 x^2	0.995	29.3
Cinnamic acid	y = 1139 – 10095 x	0.998	11.55
Caffeic acid	y = 433.1 – 558.4	0.998	4.4
Caffeic acid phenyl ester (CAPE)	y = 121.8 – 565.1 x	0.999	23.3
(+)-Catechin	y = 1460 – 2538 x	0.998	3.1
Ethyl gallate	y = 976.8 – 6209 x	0.998	5.6
Chlorogenic acid	y = 10531 – 57618 x	0.996	3.16
Kaempferide	y = 1296 – 6160 x	0.997	24.31
Naringenin	y = 3146 – 7237 x	0.998	16.04
p-Coumaric acid	y = 971.3 – 6661 x	0.997	6.51
Protocatechuic acid	y = 414.6 – 2985 x	0.997	2.80
Ferulic acid	y = 2811 – 28884 x	0.997	7.47
Rutin	y = 840.7 – 3036 x	0.997	6.46
Vanillin	y = 9927 – 72786 x	0.998	6.51
Vanillic acid	y = 20015 – 3631 x + 0.4320 x^2	0.996	4.57

Table 2: Concentration in *μ*g/g of dry weight peel (DWP) and relative standard deviation (RSD) of the phenolic compounds in orange peel

Phenolic	Concentration (μg/g DWP)	RSD (%)
Acacetin	2.34	2.0
Apigenin	44.6	3.6
Artepillin C	3.13	10.6
Caffeic acid	43.3	8.8
CAPE	17.3	7.7
(+)-Catechin	23.1	14.2
Chrologenic acid	5.01	4.8
Cinnamic acid	183.0	11.7
Ethyl gallate	116.0	8.8
Ferulic acid	316.0	12.6
Kaempferide	35.4	5.0
Naringenin	220.7	8.7
p-Coumaric acid	957.4	11.4
Protocatechuic acid	326.3	9.1
Rutin	1248.3	7.3
Vanillin	89.8	8.1
Vanillic acid	112.2	10.2

Table 3: Effect of CSMe on the intake of food and water in high-fat diet-fed STZ-induced diabetic rats

Groups	Food intake (g/rat/day)		Water intake (mL/rat/day)	
	Day 0	Day 30	Day 0	Day 30
Normal control	13.6 ± 2.9	16.2 ± 4.1	77.8 ± 4.1	82.6 ± 5.1
Diabetic control	43.4 ± 9.2[a]	58.6 ± 8.8[a]	151.6 ±11.2[a]	182.6 ± 10.2[a]
Diabetic + CSMe (50 mg/kg)	38.6 ± 5.4[a]	27.9 ± 6.1[a,b]	144.5 ± 9.1[a]	111.9 ± 10.4[a,b]
Diabetic + CSMe (100 mg/kg)	39.8 ± 7.2[a]	23.1 ± 5.1[a,b]	145.7 ± 8.6[a]	91.1 ± 8.4[a,b]
Diabetic + Metformin (100 mg/kg)	42.9 ± 8.1[a]	22.1 ± 4.7 [a,b]	143.6 ± 7.9[a]	95.9 ± 8.4[a,b]

The values indicate the mean ± SEM of six rats per group

[a]$P < 0.05$, compared with normal control values;

[b]$P < 0.05$, compared with diabetic control values.

Table 4: Effect of CSMe on OGTT in high-fat diet-fed STZ-induced diabetic rats

Groups	Blood glucose level (mg/dL)			
	0 min	30 min	60 min	120 min
Normal control	134.9 ± 6.2	176.5 ± 5.1	175.4 ± 6.2	141.3 ± 6.8
Diabetic control	323.8 ± 12.8[a]	382.6 ± 7.4[a]	394.2 ± 10.2[a]	326.3 ± 12.4[a]
Diabetic + CSMe (50 mg/kg)	222.8 ± 7.8[a,b]	283.6 ± 7.9[a,b]	241.9 ± 11.4[a,b]	232.5 ± 13.1[a,b]
Diabetic + CSMe (100 mg/kg)	231.9 ± 7.9[a,b]	275.8 ± 8.8 [a,b]	238.6 ± 12.27 [a,b]	235.1 ± 6.8[a,b]
Diabetic + Metformin (100 mg/kg)	235.4 ± 10.1[a,b]	276.5 ± 10.9[a,b]	240.6 ± 10.6 [a,b]	231.9 ± 8.4[a,b]

The values indicate the mean ± SEM of six rats per group

[a]$P < 0.05$, compared with normal control values;

[b]$P < 0.05$, compared with diabetic control values.

Table 5: Effect of CSMe on ITT in high-fat diet-fed STZ-induced diabetic rats

Groups	Blood glucose level (mg/dL)		
	0 min	30 min	60 min
Normal control	135.8 ± 4.2	105.8 ± 6.3	102.5 ± 5.2
Diabetic control	324.2 ± 12.8[a]	337.9 ± 9.4[a]	340.5 ± 8.2[a]
Diabetic + CSMe (50 mg/kg)	142.5 ± 9.3[b]	112.8 ± 8.1[b]	122.8 ± 7.6[b]
Diabetic + CSMe (100 mg/kg)	122.9 ± 5.5[b]	106.8 ± 9.7[b]	116.8 ± 7.5[b]
Diabetic + Metformin (100 mg/kg)	132.5 ± 7.4[b]	108.5 ± 8.6[b]	118.6 ± 6.2[b]

The values indicate the mean ± SEM of six rats per group

[a]$P < 0.05$, compared with normal control values;

[b]$P < 0.05$, compared with diabetic control values.

Table 6: Effect of CSMe on FBG in high-fat diet-fed STZ-induced diabetic rats

Groups	FBG level (mg/dL)			
	Day 0	Day 14	Day 21	Day 28
Normal control	107.2 ± 6.4	123.8 ± 9.2	132.8 ± 4.6	135.9 ± 8.4
Diabetic control	274.8 ± 6.2[a]	318.5 ± 9.5[a]	328.8 ± 10.2[a]	342.9 ± 11.6[a]
Diabetic + CSMe (50 mg/kg)	283.2 ± 14.2[a]	236.1 ± 7.1[a,b]	155.6 ± 10.7[a,b]	124.2 ± 8.6[b]
Diabetic + CSMe (100 mg/kg)	290.6 ± 8.8[a]	228.5 ± 6.8[a,b]	142.8 ± 9.9[b]	128.8 ± 4.8[b]
Diabetic + Metformin (100 mg/kg)	292.6 ± 6.8[a]	230.6 ± 8.7[a,b]	149.9 ± 10.4[b]	129.6 ± 8.2[b]

The values indicate the mean ± SEM of six rats per group

[a]$P < 0.05$, compared with normal control values;

[b]$P < 0.05$, compared with diabetic control values.

Table 7: Effect of CSMe on body weight in high-fat diet-fed STZ-induced diabetic rats

Groups	Body weight (g)			
	Day 0	Day 14	Day 21	Day 28
Normal control	186.8 ± 12.2	188.2 ± 13.8	192.8 ± 13.6	197.6 ± 14.8
Diabetic control	192.8 ± 10.8	217.9 ± 13.5[a]	228.8 ± 14.1[a]	237.8 ± 12.2[a]
Diabetic + CSMe (50 mg/kg)	197.4 ± 14.8	210.5 ± 9.8[a]	218.6 ± 12.2[a]	214.2 ± 12.9[a]
Diabetic + CSMe (100 mg/kg)	181.6 ± 12.1	208.4 ± 10.2[a]	213.6 ± 14.2[a]	219.5 ± 10.8[a]
Diabetic + Metformin (100 mg/kg)	202.9 ± 8.2[a]	217.4 ± 13.2[a]	222.7 ± 12.6[a]	216.6 ± 11.2[a]

The values indicate the mean ± SEM of six rats per group

[a]$P < 0.05$, compared with normal control values.

Table 8: Effect of CSMe on plasma insulin and HOMA-IR in high-fat diet-fed STZ-induced diabetic rats

Groups	Plasma insulin (µU/mL)		HOMA-IR	
	Day 0	Day 28	Day 0	Day 28
Normal control	16.1 ± 1.2	15.8 ± 0.7	4.3 ± 0.6	5.4 ± 0.6
Diabetic control	20.9 ± 0.7[a]	25.8 ± 1.3[a]	14.6 ± 2.2[a]	21.4 ± 1.4[a]
Diabetic + CSMe (50 mg/kg)	21.8 ± 0.8[a]	16.8 ± 1.2[b]	15.4 ± 1.2[a]	5.8 ± 0.9[b]
Diabetic + CSMe (100 mg/kg)	22.0 ± 1.6[a]	14.8 ± 0.5[b]	15.6 ± 1.6[a]	5.4 ± 0.6[b]
Diabetic + Metformin (100 mg/kg)	20.7 ± 1.4[a]	15.9 ± 0.5[b]	14.9 ± 1.6[a]	5.2 ± 0.8[b]

The values indicate the mean ± SEM of six rats per group

[a]$P < 0.05$, compared with normal control values;

[b]$P < 0.05$, compared with diabetic control values.

Figure captions

Fig. 1. Total ion chromatogram of methanol extract from *Citrus sinensis* fruit peel (CSMe) (A); chromatogram obtained in selected reaction monitoring (Quantization Transition) mode for pure standards (B)

Figs. 2 & 3. Chemical structures of phenolic compounds identified and quantified from methanol extract from *Citrus sinensis* fruit peel (CSMe).

Fig. 4. Effect of CSMe on TC (A), TG (B), LDL-c (C), and HDL-c (D) in high-fat diet-fed STZ-induced diabetic rats. The bar represented the mean ± SEM of six rats per group.

[a] compared with normal control group ($P < 0.05$); [b] compared with diabetic control group ($P < 0.05$).

Fig. 5. Effect of CSMe on SGOT (A), SGPT (B), ALP (C), urea (D), and creatinine (E) in high-fat diet-fed STZ-induced diabetic rats. The bar represented the mean ± SEM of six rats per group.

[a] compared with normal control group ($P < 0.05$); [b] compared with diabetic control group ($P<0.05$).

Fig. 6. Histopathological changes in the pancreatic islet tissues of experimental rats (H & E, scale Bar: 50 µm, 40×)

(A) Normal control: H & E-stained sections of the pancreas of normal control rats. Yellow arrows indicate the normal islets of Langerhans

(B) Diabetic control: Pancreatic section of high-fat diet-fed streptozotocin (STZ)-induced diabetic rats. Fewer islets of Langerhans and β-cells are seen (black arrows)

(C, D) Diabetic + (CSMe; 50 and 100 mg/kg): Pancreatic sections of diabetic rats treated with CSMe. Normal pancreatic islets of Langerhans and enhanced numbers of β-cells are seen (yellow arrows)

(E) Diabetic + Metformin (100 mg/kg): Pancreatic sections of diabetic rats treated with metformin. Increased numbers of islets of Langerhans and appropriate proportions of β-cells are seen (yellow arrows)

Fig. 7. Histological interpretations of adipose tissues of experimental rats (H & E, scale bar = 50 µm, 40×)

(A) Normal control: H & E-stained sections of normal control rat indicating the usual and regular distribution of cellular types in adipose tissue

(B) Diabetic control: Tissue sections of high-fat diet-fed STZ-induced diabetic rats showing regressed and unusual distribution of cellular types in adipose tissue (C, D) Diabetic + (CSMe; 50 and 100 mg/kg) : Stained sections of diabetic rats treated with CSMe indicating normal and regular distributions of cellular types in adipose tissue (E) Diabetic + Metformin (100 mg/kg): Section of diabetic rats treated with metformin showing usual distribution of cellular types in adipose tissue

Fig. 8. Light micrograph showing the intensity of immunostaining for insulin containing β-cells in the islets of Langerhans (scale bar = 50 µm, 40×)

(A) Normal control: Islet tissue section of normal control rats showing positive insulin containing β-cells

(B) Diabetic control: Islet tissue sections of high-fat diet-fed STZ-induced diabetic rats showing decreased positive staining for insulin containing β-cells

(C, D) Diabetic + (CSMe; 50 and 100 mg/kg) : Islet tissue sections of diabetic rats treated with CSMe showing increased and adequate positive insulin containing β-cells

(E) Diabetic + Metformin (100 mg/kg): Islet tissue sections of diabetic rats treated with metformin showing better and sufficient positive insulin containing β-cells

Fig. 9. Histogram showing intensity of immunostaining for insulin containing β-cells in the islets of Langerhans

(A) Normal control, (B) Diabetic control, (C) Diabetic + CSMe (50 mg/kg), (D) Diabetic + CSMe (100 mg/kg), (E) Diabetic + Metformin (100 mg/kg)

Bars represent the mean ± SEM of six rats per group

[a] compared with normal control group ($P < 0.05$); [b] compared with diabetic control group ($P<0.05$).

Fig. 10A. Effects of CSMe on the mRNA expressions of PPARγ, GLUT4, IR, and β-actin in adipose tissue of experimental animals. (Lane 1) Normal control, (Lane 2) Diabetic control, (Lane 3) Diabetic + CSMe (50 mg/kg), (Lane 4) Diabetic + CSMe (100 mg/kg).

The bars represent the mean ± SEM of three independent experiments.

[a] compared with normal control group ($P < 0.05$); [b] compared with diabetic control group ($P<0.05$).

Fig. 10B. Effects of CSMe on the protein expressions of PPARγ, GLUT4, IR, and β-actin in the adipose tissue of experimental animals. (Lane 1) Normal control, (Lane 2) Diabetic control, (Lane 3) Diabetic + CSMe (50 mg/kg), (Lane 4) Diabetic + CSMe (100 mg/kg).

The bars represented the mean ± SEM of three independent experiments.

[a] compared with normal control group ($P < 0.05$); [b] compared with diabetic control group ($P<0.05$).

A

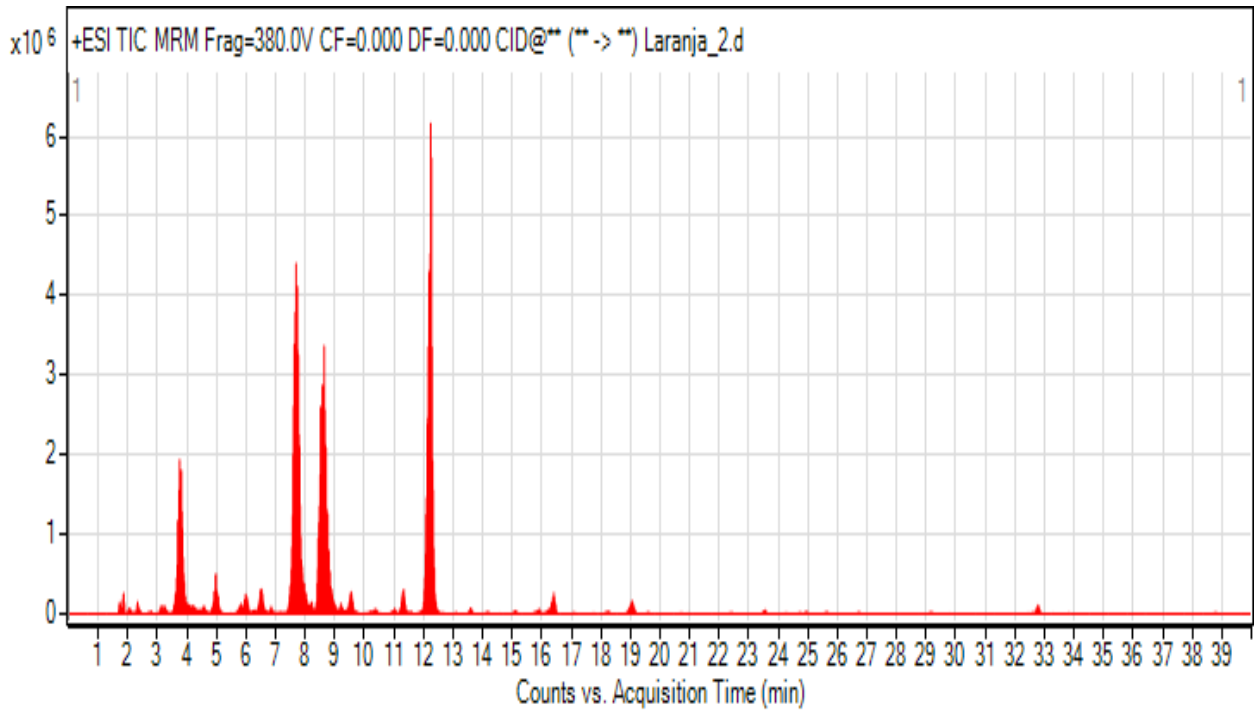
x10 6
+ESI TIC MRM Frag=380.0V CF=0.000 DF=0.000 CID@** (** -> **) Laranja_2.d
Counts vs. Acquisition Time (min)

B

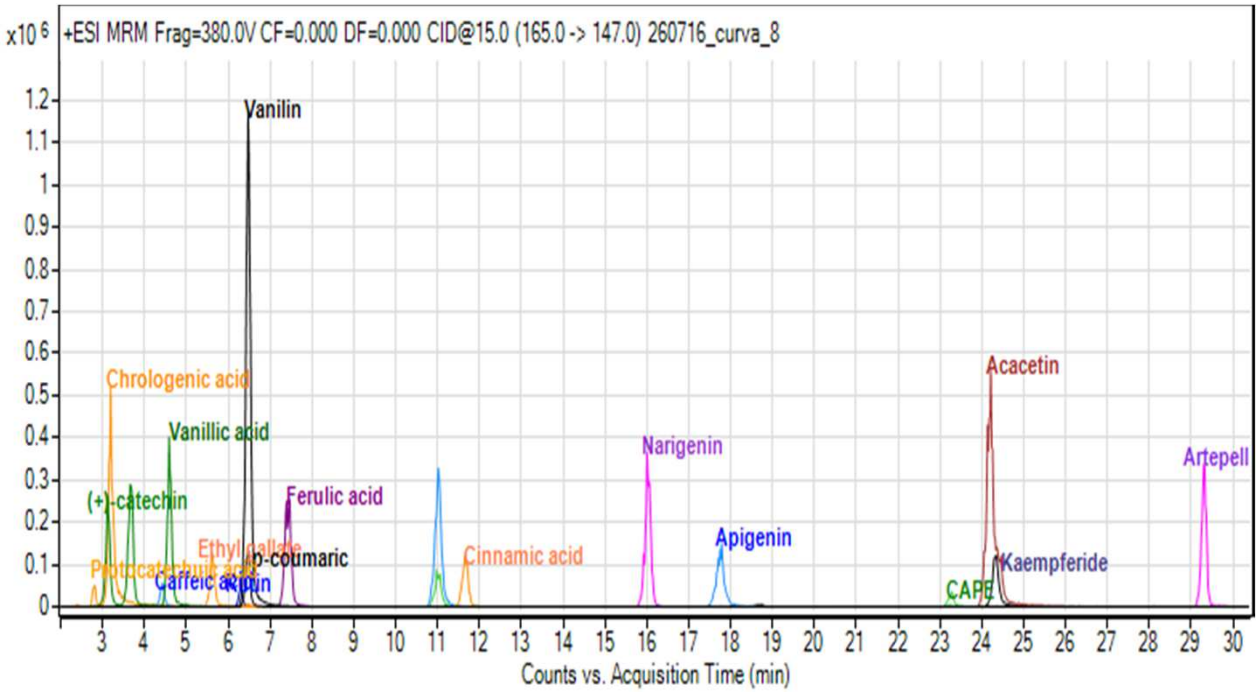
x10 6
+ESI MRM Frag=380.0V CF=0.000 DF=0.000 CID@15.0 (165.0 -> 147.0) 260716_curva_8
Vanilin
Chrologenic acid
Vanillic acid
(+)-catechin
Ferulic acid
Ethyl gallate
p-coumaric
Protocatechuic acid
Caffeic acid
Apigenin
Cinnamic acid
Narigenin
Acacetin
Kaempferide
CAPE
Artepell
Counts vs. Acquisition Time (min)

Fig. 1.

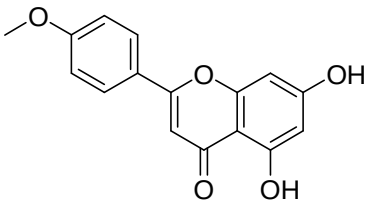

Acacetin

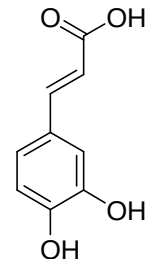

Caffeic acid

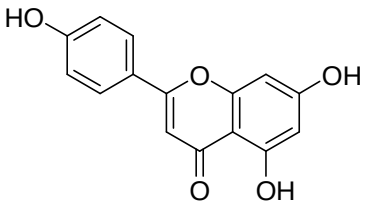

Apigenin

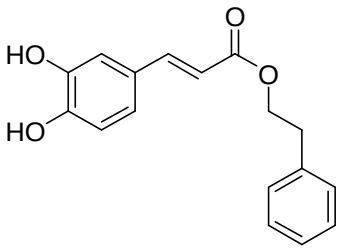

Caffeic acid phenyl ester (CAPE)

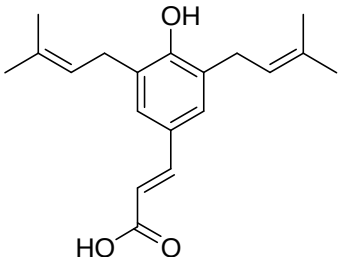

Artepillin C

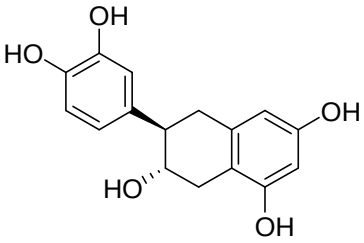

(+) - catechin

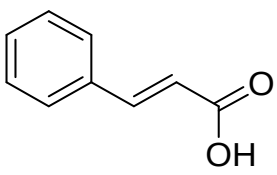

Cinnamic acid

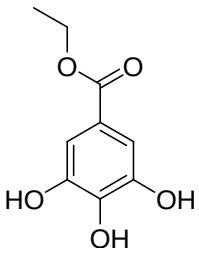

Ethyl gallate

Fig. 2.

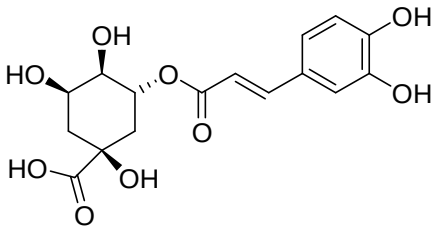

Chlorogenic acid

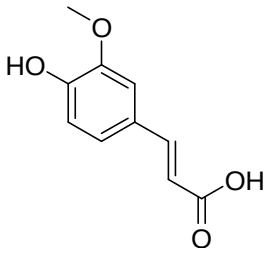

Ferulic acid

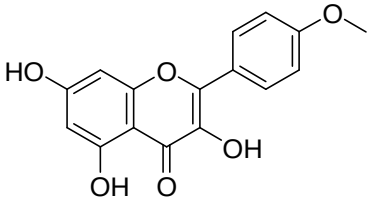

Kaempferide

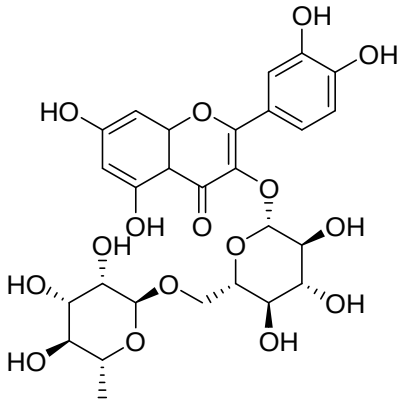

Rutin

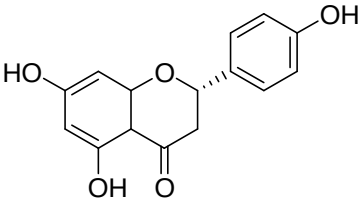

Naringenin

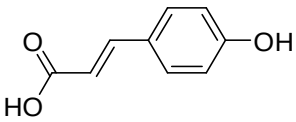

p-coumaric acid

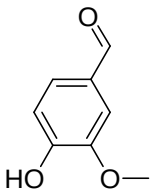

Vanillin

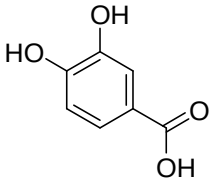

Protocatechuic acid

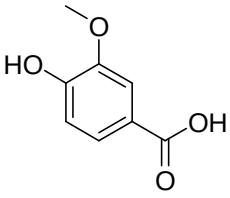

Vanillic acid

Fig. 3.

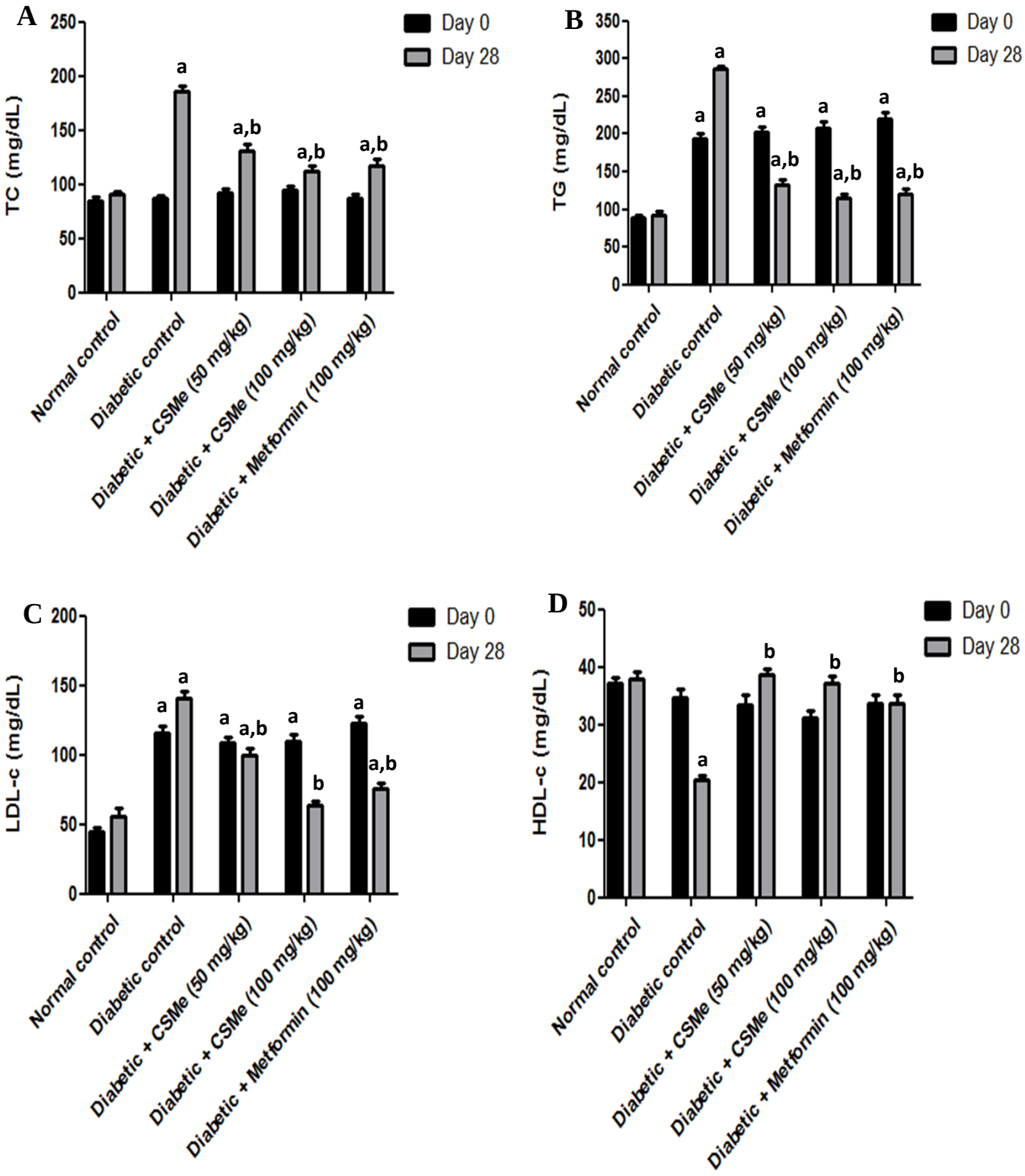
A
TC (mg/dL)
Day 0
Day 28
B
TG (mg/dL)
C
LDL-c (mg/dL)
D
HDL-c (mg/dL)
Normal control
Diabetic control
Diabetic + CSMe (50 mg/kg)
Diabetic + CSMe (100 mg/kg)
Diabetic + Metformin (100 mg/kg)

Fig. 4.

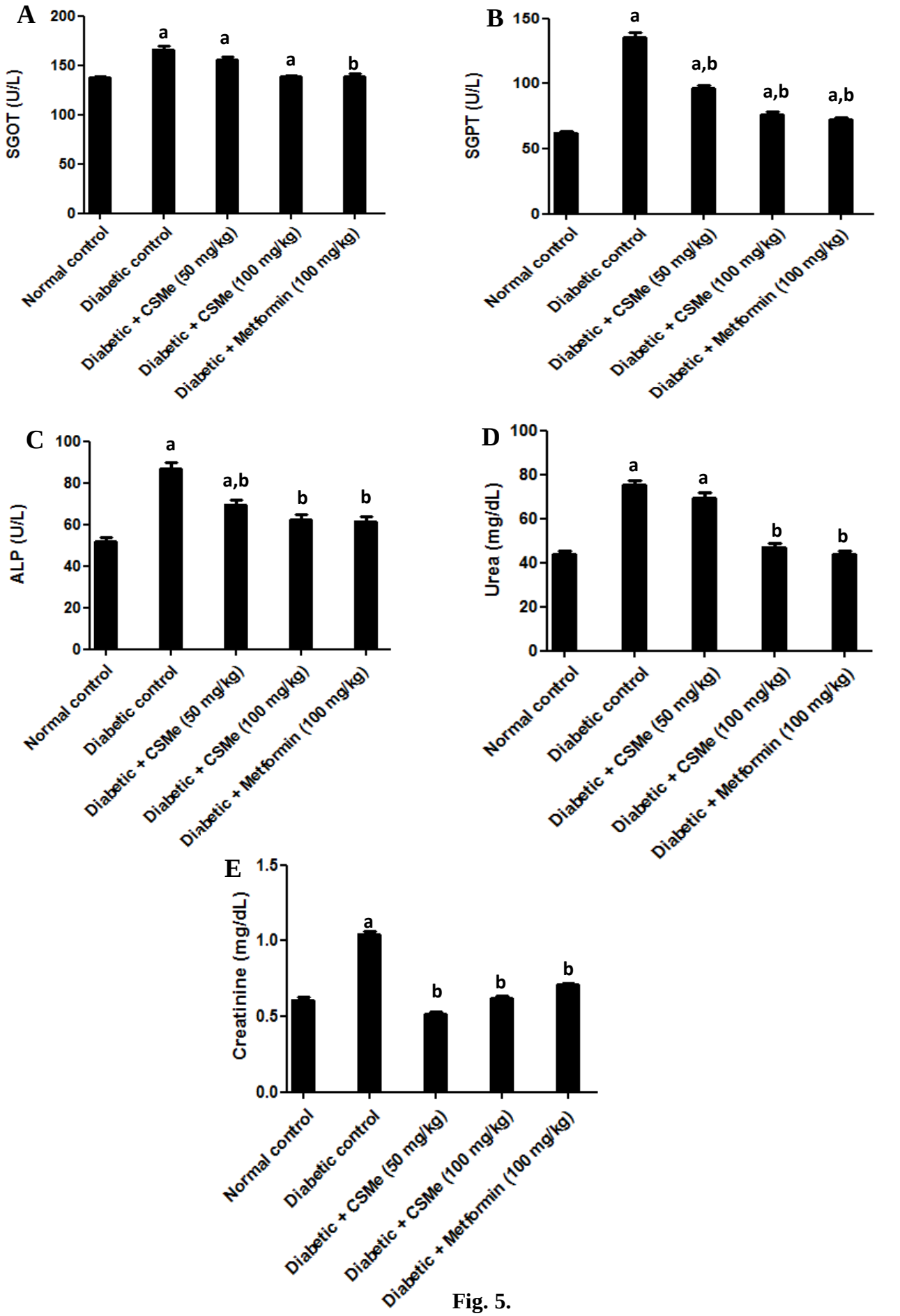
A
SGOT (U/L)
200
150
100
50
0
a
a
a
b
B
SGPT (U/L)
150
100
50
0
a
a,b
a,b
a,b
C
ALP (U/L)
100
80
60
40
20
0
a
a,b
b
b
D
Urea (mg/dL)
100
80
60
40
20
0
a
a
b
b
E
Creatinine (mg/dL)
1.5
1.0
0.5
0.0
a
b
b
b
Normal control
Diabetic control
Diabetic + CSMe (50 mg/kg)
Diabetic + CSMe (100 mg/kg)
Diabetic + Metformin (100 mg/kg)

Fig. 5.

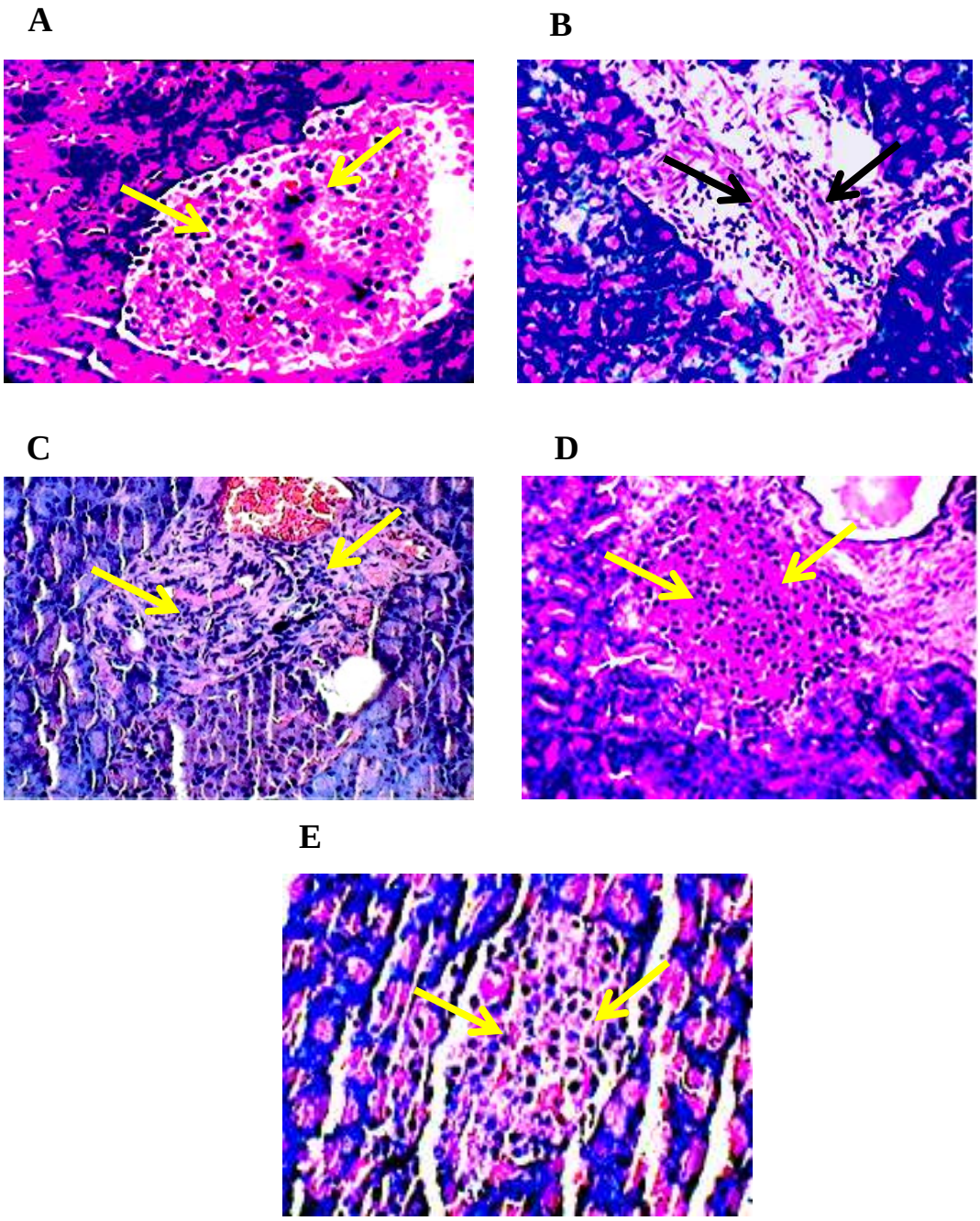

Fig. 6.

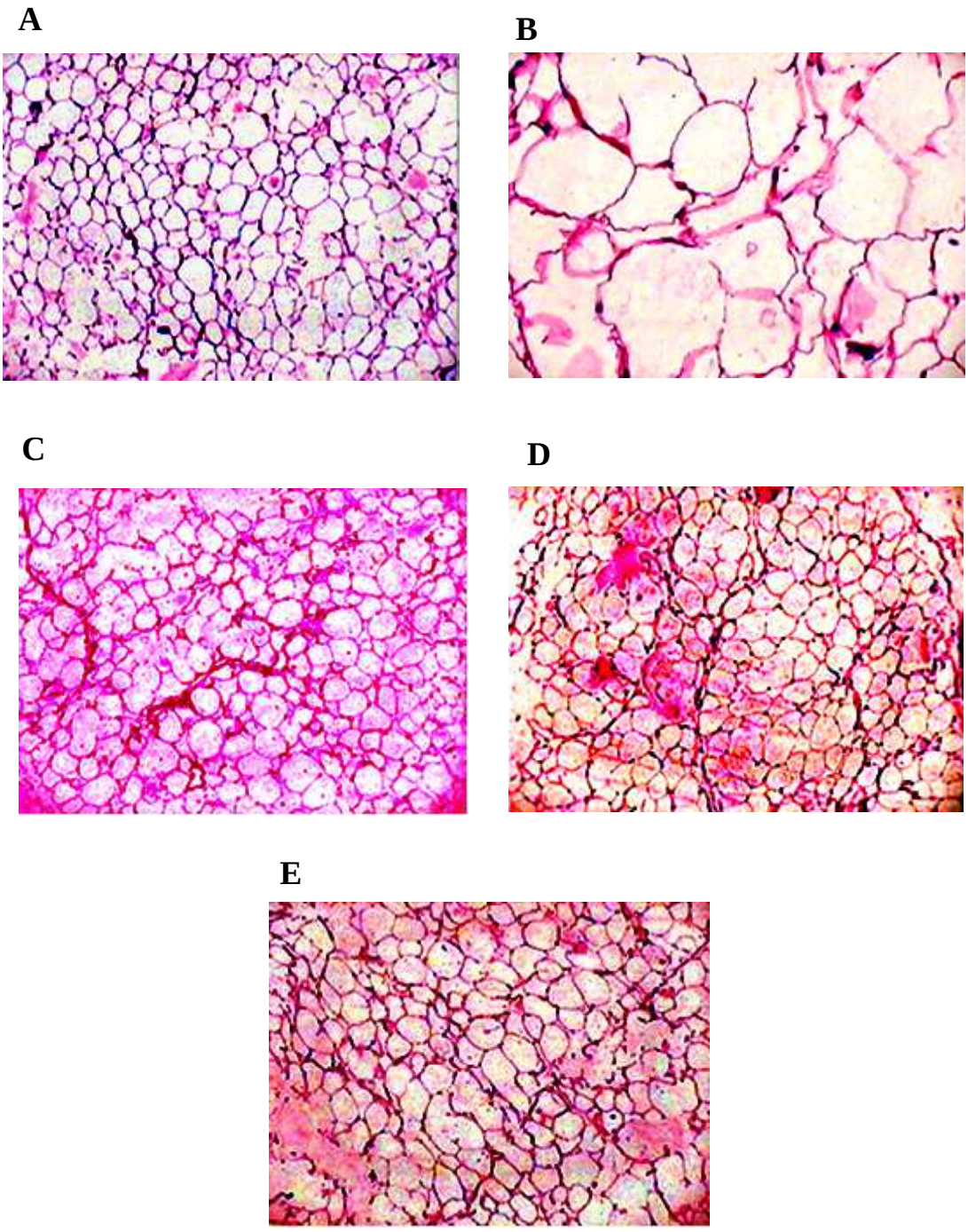

Fig. 7.

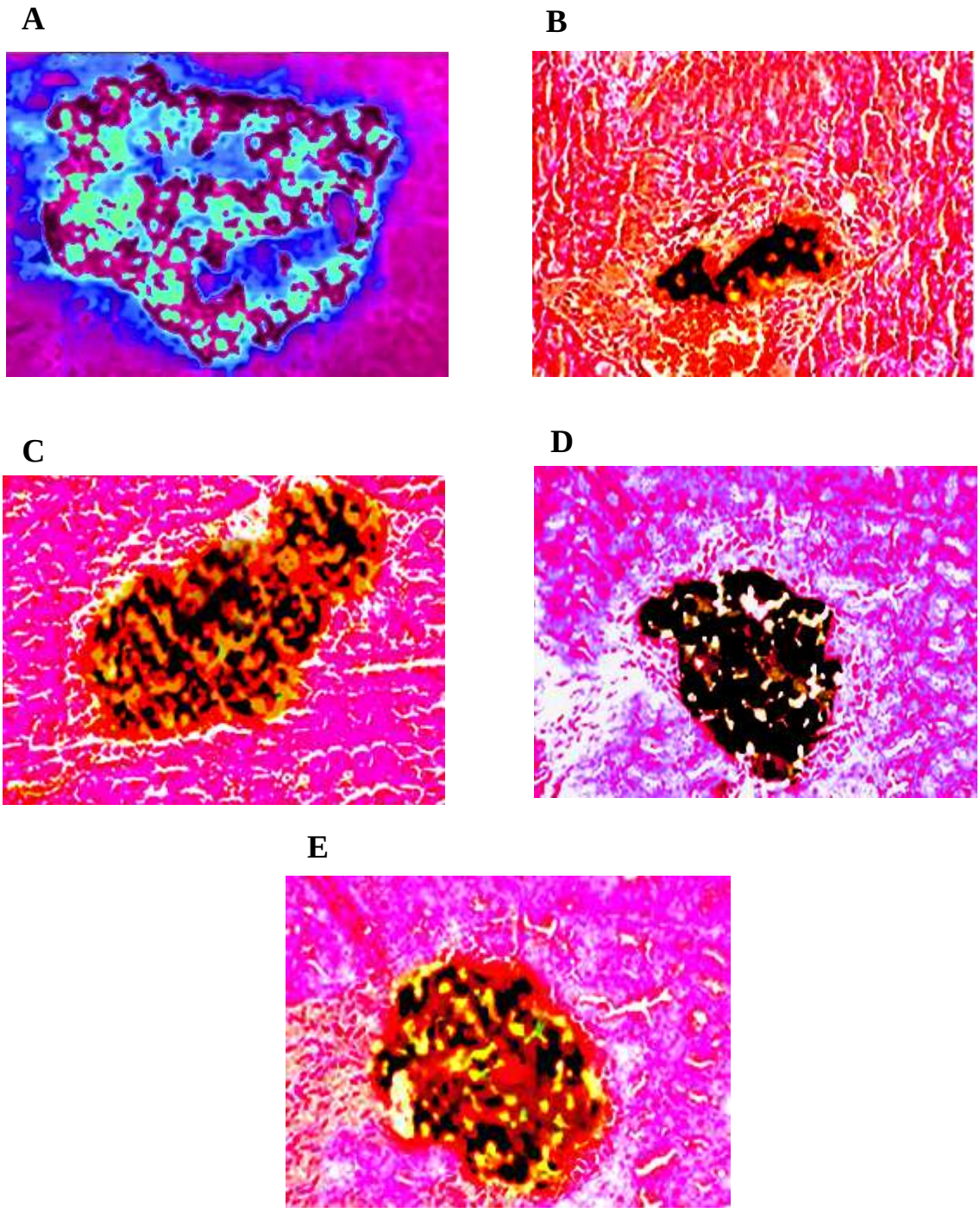

Fig. 8.

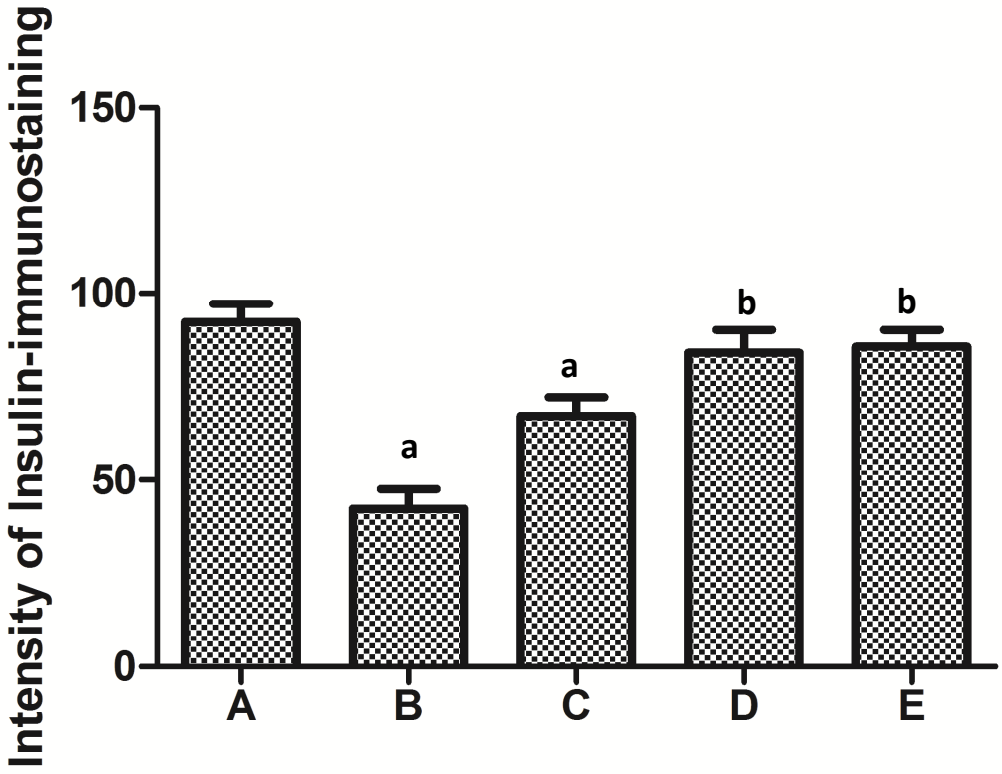
Intensity of Insulin-immunostaining
150
100
50
0
a
a
b
b
A
B
C
D
E

Fig. 9.

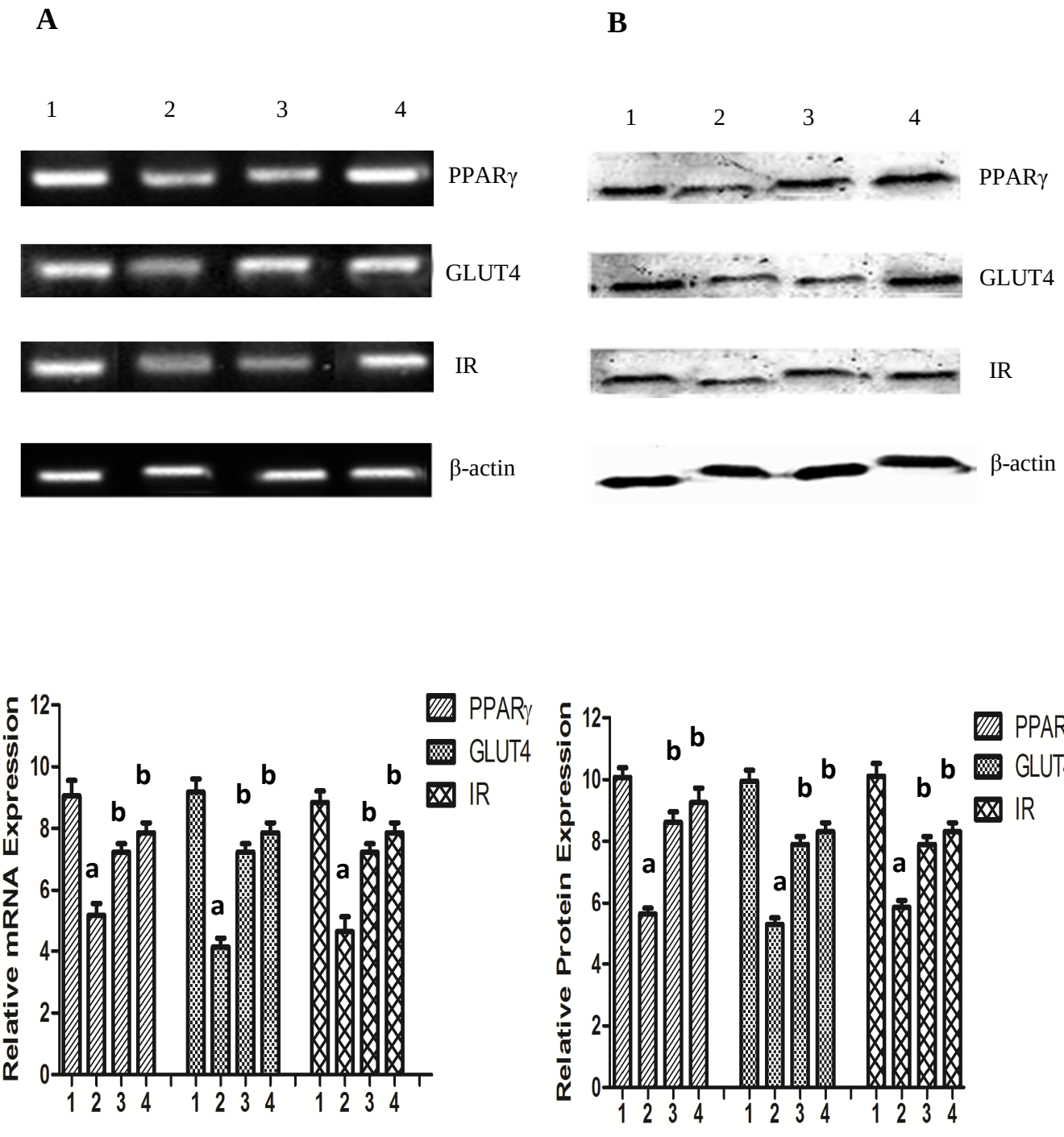
A
1
2
3
4
PPARγ
GLUT4
IR
β-actin
B
1
2
3
4
PPARγ
GLUT4
IR
β-actin
Relative mRNA Expression
PPARγ
GLUT4
IR
Relative Protein Expression
PPARγ
GLUT4
IR

Fig. 10.

Highlights

- *Citrus sinensis* peel methanol extract lowered blood glucose level in diabetic rats
- *Citrus sinensis* peel contained fine concentrations of phenolic compounds
- *Citrus sinensis* peel possessed cytoprotective action
- *Citrus sinensis* peel promoted insulin receptor signaling